Inorganic Chemistry
Award Article

*Inorg. Chem.* **2010**, *49*, 13–28 **13**
DOI: 10.1021/ic901305g

# Exploratory Synthesis: The Fascinating and Diverse Chemistry of Polar Intermetallic Phases†

**John D. Corbett***

*Department of Chemistry and Ames Laboratory, Iowa State University, Ames, Iowa 50011*

Received July 6, 2009

Exploratory synthetic adventures regarding the inorganic chemistry of polar intermetallic phases have proven to be especially productive of novel compositions, new and unprecedented structures, and unusual bonding regimes. Reactions of diverse elements with widely different electronegativities allow the definition of two opposed classes of products: polycationic or polyanionic clusters or networks of metals paired with the corresponding monatomic anions or cations. These can be usefully viewed as intermetallic "salts", redox products of simpler neutral intermetallic systems but with widely different factors governing their stabilities. Thus, combinations of rare-earth metals alone or with late transition metals form a novel variety of polymetal network structures with relatively isolated telluride (or halide) spacer anions. Similarly, extensions of traditional Zintl phases of the alkali or alkaline-earth metals from the later p elements to the earlier *triels*, Ga−Tl especially, yield many new and elegant polyanionic structures. The substitution or addition of still earlier p or late d metal components produces still electron-poorer and more condensed polar intermetallic phases with increasingly delocalized bonding, higher coordination numbers, and more unusual structures and bonding. These discoveries have also led to new approaches: electronic tuning via band calculations to generate new families of quasicrystals and their crystalline approximants with their characteristic structural regimes and regularities. Gold as a substituent generates particularly novel bonding in arrays of mixed metals or polygold anionic networks.

## Forward

For someone who has spent most of his scientific career on the synthesis and characterization of new solid-state compounds around the periodic table, the receipt of the 2008 F. Albert Cotton Award in Synthetic Inorganic Chemistry is a wonderful accomplishment and honor. That award address stayed rather close to the new discoveries achieved since 2000 and my previous ACS award,[1] and this transcription does likewise, addressing principally new and marvelous intermetallic materials, notwithstanding, "First Comes the Synthesis",[2] that is, the need for a high yield of a clearly identified phase and composition. The problems and precautions that need to be faced or taken regarding this vital first step will not be related here but left to "the fine print". Practitioners will still need to consider, even be suspicious about, side reactions, impurity stabilization, nonstoichiometry, complex phase relationships, and other potential problems. "Neat" reactions at elevated temperatures have been employed throughout because of the better control of yields and purities achieved.

† This article is based on J. D. Corbett's address upon receipt of the 2008 American Chemical Society's F. Albert Cotton Award in Synthetic Inorganic Chemistry sponsored by the F. Albert Cotton Endowment Fund.

*To whom correspondence should be addressed. E-mail: jcorbett@iastate.edu or jdc@ameslab.gov.

(1) Corbett, J. D. *Inorg. Chem.* **2000**, *39*, 5178.
(2) Corbett, J. D. *Acc. Chem. Res.* **1981**, *14*, 239.

## I. Intermetallic Phases

This presentation has to do with the chemistry, structures, and properties in a relatively unfamiliar area, phases or compounds for which a simple description is "intermetallic". Literally, this applies to compounds between two or more elements that are each metals, with this designation simply following the negative temperature dependence of the electronic conductivity of each. The usage is rather loose, not distinguishing whether the parents are simple s or d metals or metalloids (~p metals) or even whether the products themselves are metallic; even silicides, etc., of one or more metals may also be called intermetallics if their conduction fits, or is presumed to.

Several general conditions apply to these systems. Their attributes are as follows:

- Unique to the dense solid (or liquid) state
- Equilibrium phases, as opposed to metastable materials, in accordance with the usual synthetic routes at elevated temperatures
- A lack of simple bonding or valence rules and closed-shell states, in contrast to most molecular and simple semiconductor materials
- Generally delocalized bonding of the valence electrons, which is natural in the presence of a surplus of valence orbitals and, accordingly, high coordination numbers about most atoms


Published on Web 12/07/2009

- Widely diverse in the details of the bonding, depending in general ways on the nature of the elements involved as well as on the structures, stoichiometries, and other factors (the physical properties likewise vary widely)
- Certain systems that may still exhibit some characteristic but unusual valence rules and thereby approach closed-shell configurations (pseudogaps) at certain compositions, often reflecting electronic effects that are not well understood (more examples and some regularities will certainly be found in this area)

As we will show, there *is* chemistry *in* intermetallic phases. It is not by accident that we have chosen to "fish" among a particular subset of these, the *polar intermetallic phases*. Such materials are widely distributed over the periodic table, and so even the sheer number of possibilities can be a bit overwhelming.[3]

## II. New Intermetallic Classes via the Reduction or Oxidation of Metal Systems

Conceptually, a useful way to get into new phase space and to avoid the native stability restrictions among neutral products in simple intermetallic systems is via *oxidation* or *reduction* of these. This process yields polyatomic "salts" of metal networks that are now either cationic or anionic in the formal sense of oxidation states and are paired with more or less simple monoanions or cations, respectively. The stabilities of such products and structures are in most cases governed by disproportionation reactions. This classification scheme has, in fact, evolved from the results of diverse synthetic explorations rather than out of conscious thought and expectations.

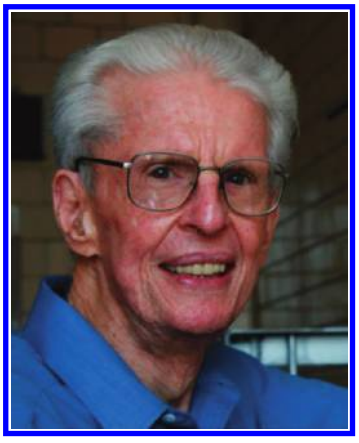

John D. Corbett was born in Yakima, WA, in 1926. After service in V-12 (NROTC) units in the midwest during World War II, he went on to finish his B.S. (1948) and Ph.D. (1952) degrees at the University of Washington, the latter with Norman W. Gregory in physical chemistry. He has been associated with the Department of Chemistry and Ames Laboratory (DOE) at Iowa State University ever since, where he is presently Professor of Chemistry, Distinguished Professor in the College of Liberal Arts and Sciences, and Senior Chemist. He has during the interim also served as Chairman of the Department of Chemistry (1968−1973) and as Program Director and Division Chief in Ames Laboratory. The general long-term focus of his research program has been wide-ranging exploratory synthesis along metal−salt interfaces and related intermetallic systems coupled with structural and bonding characterization and analysis. Corbett earlier received the ACS Awards in Inorganic Chemistry (1986) and for Distinguished Service in the Advancement of Inorganic Chemistry (2000), an Alexander von Humboldt Senior Scientist Award, the Frank H. Spedding Award, and two Department of Energy Awards in Materials Chemistry. He is a member of the National Academy of Sciences. Photograph courtesy of Holly Anderson.

**A. Oxidation to Polycationic Networks with Simple Anions.** This pertains to a family of stable structures of early, or early plus late, transition metals in which polycationic networks are partnered with limited amounts of simple nonmetal anions. The strengths of homoatomic metal−metal bonds among the early-to-mid transition metals in lower oxidation states allow access to many metal−metal-bonded products when only moderate oxidation is employed, generally in the presence of simple $np^6$ monoanions, often halide. These phases are, of course, not composed of only metallic elements, but there is little to no doubt that most examples with extended cationic networks are metallic (baring unexpected special electronic stabilities). The parents of this class are the longer known discrete clusters in binary phases such as $(Ta_6Cl_{12})^{2+}(Cl^-)_2$ and the like,[4,5] and this family can be extended to a considerable variety of $Zr_6(Z)Cl_{12}{}^{n+}$ analogues when extra electrons and bonding are supplied by one of a considerable variety of interstitial atoms Z, group 8−12 transition metals in particular.[6] The last products exhibit significantly stronger bonding by virtue of the early−late-transition-metal combinations,[7] but substantially all are probably semiconductors because the characteristic clusters are isolated by layers of halide. A switch to the even-electron-poorer rare-earth elements (R) leads to fewer anions and a unique set of diverse extended aggregates that usually can be described in terms of discrete condensed clusters or polymetal frameworks (below).

**B. Reductions to Polyanionic Networks with Simple Cations.** The original examples were the classical Zintl phases, products of limited alkali-metal reduction of p elements, mainly those from groups 14−16, often in combination. The polyanionic products range from molecular anions to extended aggregates and customarily follow simple valence (octet) rules for bonding, whereas the cation partners have commonly been considered to be electron donors and simple spacers.[8] Semiconductor properties have been the expectation, but these are not always achieved with group 14 metals, the *tetrels*. The chemistry expands considerably when group 13 *triels* (Ga, In, and Tl especially) are used instead. The "Zintl border" between these two groups was the original limit assigned by Zintl, but the loss of classical bonding properties and a transition to intermetallics around this point are not so simple or direct. A great deal of new and novel intermetallic chemistry evolves when still earlier elements are also introduced, including the late and heavier

(3) DiSalvo, F. J. *Pure Appl. Chem.* **2000**, *72*, 1799.

(4) Schaefer, H.; Schnering, H.-G. *Angew. Chem.* **1964**, *76*, 833.
(5) Perrin, C. In *Metal Clusters in Chemistry*; Braunstein, P., Oro, L. A., Raithby, P. R., Eds.; Wiley-VCH: Weinheim, Germany, 1999; Vol. *3*, p 1563.
(6) (a) Corbett, J. D. *J. Alloys Compd.* **1995**, *229*, 10. (b) Corbett, J. D. *J. Alloys Compd.* **2006**, *418*, 1.
(7) Brewer, L.; Wengert, P. R. *Metall. Trans.* **1973**, *4*, 83.
(8) Kauzlarich, S., Ed. *Chemistry, Structure and Bonding of Zintl Phases and Ions*; VCH Publishers: New York, 1996.

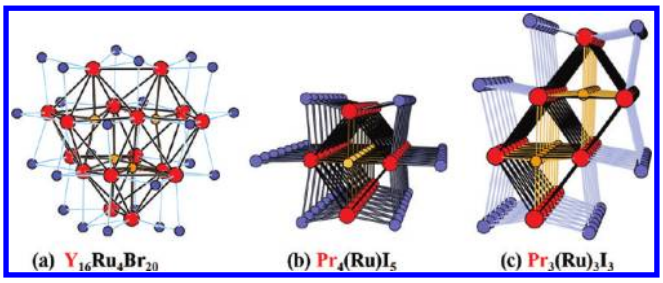


**Figure 1.** Three examples of condensed rare-earth-metal cluster halides centered by the heterometal Ru: (a) $Y_{16}(Ru)_4$ metal core (red and orange) in $Y_{16}Ru_4Br_{20}$, conceptually from a 2 + 2 addition of $Y_6Ru$ clusters; (b) portion of a single chain in $Pr_4(Ru)I_5$ from condensation of hypothetical $Pr_6RuI_8$ clusters via shared *trans*-Pr−Pr edges; (c) double chain in $Pr_3(Ru)I_3$ from side-by-side condensation of two chains as found in b. R metals are red, Ru orange, and halide blue.

d metals, Au especially. We will start with the divergence at the triels.

## III. Polymetal Networks with Simple Anions

Compared with octahedral zirconium cluster halides, for which the clusters are all stabilized by interstitial atoms, the electron-poorer rare-earth-metal (R) analogues naturally exhibit greater degrees of condensation. (This results because roughly similar numbers of cluster-based electrons per metal atom turn out to be necessary for stability.) Thus, less oxidation of the parent metal, fewer halide counteranions, and more metal−metal condensation follow. In any case, the outer edges or faces (and sometimes vertices) of the metal aggregates are inevitably capped by halides, which, we imagine, prevent further condensation of the metal clusters or frameworks.[6] Thus, the systems are quite acidic, and "free" halide ions are accordingly rare.

For background, three types of important rare-earth-metal halide examples that contain condensed clusters are shown in Figure 1a−c. (The essential earlier details, the often-painstaking synthetic and crystallographic efforts, are omitted from the present descriptions, focusing only on the structures and bonding themselves.) The oligomeric polycation $Y_{16}Ru_4$ shown in part a, the core in $Y_{16}Ru_4X_{20}$ (X = Br, I), does not include details of the necessary capping or bridging halide functions on and between these units. The geometry, a Ru-stuffed, tetracapped, truncated tetrahedron (icosioctahedron) of Y, can alternatively be viewed as a result of a 2 + 2 condensation of four $Y_6(Ru)X_8$ (face-capped) clusters. Distortions in the oligomer suggest stronger Ru−Y bonding than that found in Ru−Pr analogues.[9] Other examples are known only with Sc or Gd. Two more common modes of condensation to semiinfinite arrays are also illustrated. $Pr_4(Ru)I_5$ in part b contains infinite cluster chains that can be viewed as the condensation product of (hypothetical) Ru-centered $Pr_6I_{12}$ (edge-bridged) octahedral clusters through sharing of both *trans*-Pr−Pr bonds in the octahedra and neighboring I atoms.[10] (Edge-bridging iodide groups on neighboring chains are also bound exo at the metal vertices in part b to complete the isolation of the metal fragment.) Smaller amounts of halogen afford the closely related $Pr_3(Ru)I_3$-like product in part c in which pairs of the previous

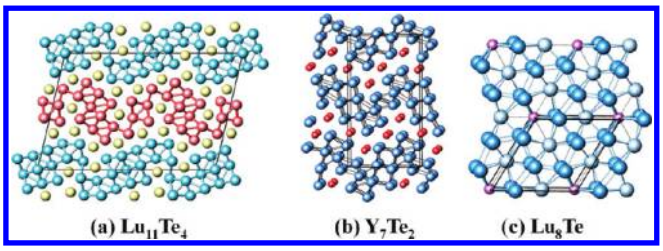


**Figure 2.** 2D and 3D condensation results among binary rare-earth-metal tellurides, all of which are infinite in projection along ~4.0 Å repeat axes. (a) $Lu_{11}Te_4$: two puckered sheets of Lu (red and blue) separated by yellow Te atoms. (b) $Y_7Te_2$: chains of (mainly) trans-edge-sharing Y octahedra along the projection that are further condensed by sharing side edges to form thin puckered layers of Y (blue) and separated by columns of isolated Te atoms (red). (c) Hexagonally packed layers of Lu in $Lu_8Te$ (blue and light blue) with lavender Lu sites in the latter substituted by Te.

single chains have been further condensed through sharing of Pr−Pr side edges.[11] In general, the dependencies of stabilities on Z are complex, varying with, among other things, the relative stabilities of *alternate* products between R and Z. More details and references appear elsewhere.[1,5,12] The variety of structural motifs discovered have well-exceeded anyone's ability to foresee them.

Curiosity and continuing questions about the range for this sort of chemistry led to a comparable exploration of the analogous monochalcogenides. Tellurium was selected, in part, because so little was known about metal-rich telluride systems beyond RTe and $R_2Te_3$ compositions. Again, roughly the same number of valence electrons per network metal atom as that in the cluster halides (~2) means about half as many monotelluride anions are necessary. The resulting R-metal substructures are accordingly much more tightly packed and three-dimensional (3D), and this alone transports us into new regions of metal-rich structures and bonding, whereas the nominal $Te^{2-}$ are commonly centered in simple bi- or tri-capped trigonal prisms of R. More novel and complex binary phases are now found than with halide and some without an interstitial metal Z.[13] It is all a matter of relative stabilities, of course.

Three unusual binary telluride structures of this type are illustrated in Figure 2a−c, and these also demonstrate how much more difficult it may be to visualize the 3D nets. Fortunately, all three are projected along short repeat axes (~4 Å, the diameter of Te), and all atoms lie on successive mirror planes at 0, $^1/_2$, 1, etc., normal to the projection. The first two can also be imagined to be built mainly of chains of condensed octahedra along the view that further share side edges, as seen in isolation in Figure 1b,c. (The shorter shared-edge connections in these octahedra are marked with lighter lines to aid visualization.) The first, $Lu_{11}Te_4$ (a), contains two distinctive infinite puckered sheets of Lu (blue and red, seen on the edge) separated by single puckered layers of Te (yellow).[14] The view in part b is of one-of-a-kind $Y_7Te_2$ with

(9) Steinwand, S. J.; Corbett, J. D. *Inorg. Chem.* **1996**, *35*, 7056. Steinwand, S. J.; Corbett, J. D.; Martin, J. D. *Inorg. Chem.* **1997**, *36*, 6413.
(10) Payne, M. W.; Dorhout, P. K.; Corbett, J. D. *Inorg. Chem.* **1991**, *30*, 1467.
(11) Payne, M. W.; Dorhout, P. K.; Kim, S.-J.; Hughbanks, T. R.; Corbett, J. D. *Inorg. Chem.* **1992**, *31*, 1389.
(12) Simon, A.; Mattausch, Hj.; Miller, G. J.; Bauhofer, W.; Kremer, R. K. In *Handbook on the Physics and Chemistry of Rare Earths*; Gschneidner, K. A., Eyring, L., Eds.; Elsevier Science Publishers: Amsterdam, The Netherlands, 1991; Vol. *15*, p 191.
(13) Corbett, J. D. In *Inorganic Chemistry in Focus II*, Meyer, G., Naumann, D., Wesemann, L., Eds.; Wiley-VCH: Weinheim, Germany, 2005; Vol. *2*, Chapter 8.
(14) Chen, L.; Xia, S.-Q.; Corbett, J. D. *Inorg. Chem.* **2005**, *44*, 3057.

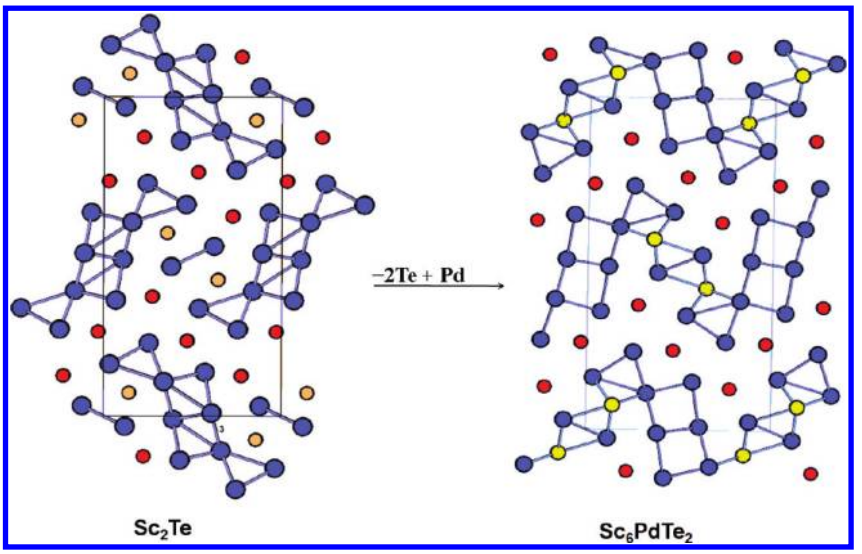


**Figure 3.** Systematic oxidative displacements of certain Te (orange) by Pd (yellow) that conceptually convert $Sc_2Te$ (left) into $Sc_6(Pd)Te_2$ (right) (both *Pnma*).

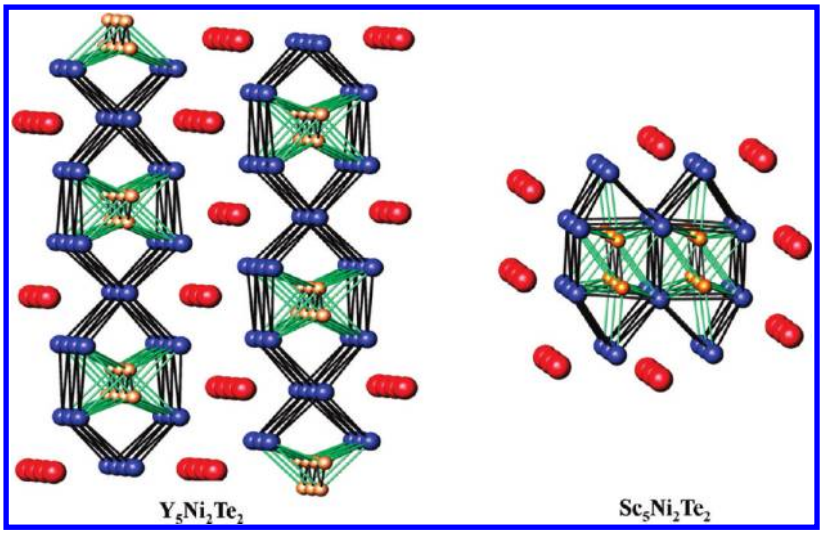


**Figure 4.** Projections of two different monoclinic $R_5Ni_2Te_2$ compounds. Both contain Ni-centered puckered hexagons of R that are condensed along the view: left, at trans apexes to yield sheets for R = Y; right, side-by-side into columns with R = Sc (interstitial Ni atoms are orange).

a similar general theme, but the idea of condensed octahedral chains along the view is clearer here with the higher proportion of R.[15] (The genesis of this result will be considered shortly.) Last, Figure 2c shows the surprising result of "doing the right experiment for the wrong reason", the structure of $Lu_8Te$. This view is normal to the simple hcp (hexagonally close-packed; *abab*...) arrangement of Lu (a-type) layers (blue) between intervening mixed Lu (light blue) and Te (lavender) layers in b-type positions. A more complex and unprecedented $Lu_7Te$ is also found nearby.[16]

The salutary effect of additional bonding between the rare-earth and late transition metals,[7] already established among the metal-rich halides (above), is realized in new chemistry and novel structures among the ternary tellurides, in large part because of their greater degrees of metal network condensation. An after-the-fact relationship between particular binary and ternary members is shown in Figure 3. The first novel discovery among the binary scandium tellurides, $Sc_2Te$ (left), consists of small condensed columns of (mostly) Sc octahedra (blue) together with separate strings of weakly bound $(Sc_2)_n$ units, all of which are separated by telluride anions (red), with these features again being semiinfinite in depth.[17] This structure is formally related to a newer family of $Sc_6ZTe_2$ phases (in the same monoclinic space group), Figure 3 (right), through the oxidative insertion of Z (e.g., Pd, yellow) for certain (the more orange) Te atoms in the former,[18] viz.,

$$4Sc_2Te + Pd \rightarrow Sc_6PdTe_2 + 2ScTe$$

Finally, this same (yellow) Z site is instead occupied by another Y in the novel structure of $Y_7Te_2$ (Figure 2b).

(15) Castro-Castro, L. M.; Chen, L.; Corbett, J. D. *J. Solid State Chem.* **2007**, *180*, 3172.
(16) Chen, L.; Corbett, J. D. *J. Am. Chem. Soc.* **2003**, *125*, 7794.
(17) Maggard, P. A.; Corbett, J. D. *Angew. Chem., Int. Ed. Engl.* **1997**, *36*, 1974.
(18) Maggard, P. A.; Corbett, J. D. *J. Am. Chem. Soc.* **2000**, *122*, 10742.

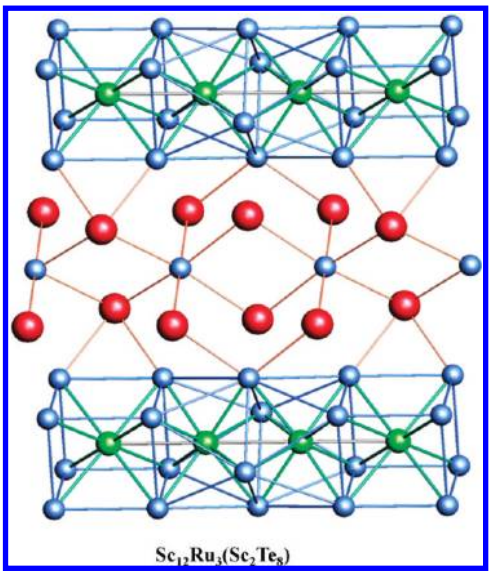


**Figure 5.** Section of the $Sc_{14}Z_3Te_8$ (Z = Ru, Os) structure that contains infinite $Sc_{12}$ chain units (blue) generated from face-sharing of alternating Sc cubes and double antiprisms, each centered by Z (green). The chains are connected via condensed, bridging $ScTe_{6/(2/3)}$ groups.

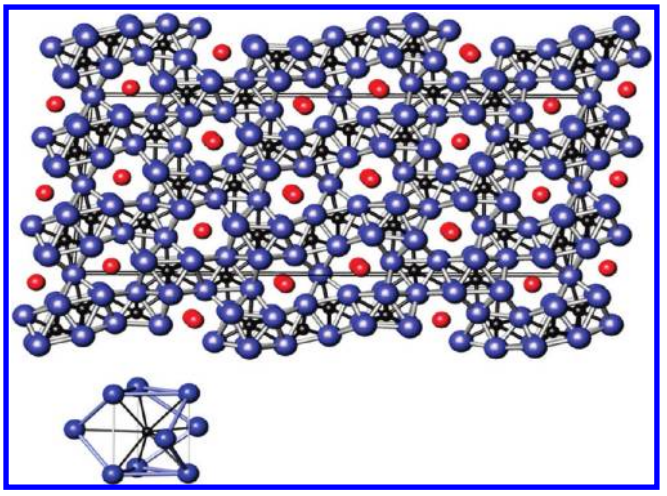

**Figure 6.** The particularly metal-rich phase $Dy_{17}Ru_6Te_3$ built of infinite columns of Ru-centered trigonal prisms of Dy (seen in the projection) that are also condensed laterally through shared Dy into a 3D network of tricapped trigonal prisms (side view of an example shown below). Te is red, Ru black, and Dy blue.

New and related structure types have recently been found for two $R_5Z_2Te_2$ polytypes with similar types of metal condensation, but they are sufficiently complex that they are presented more symbolically in Figure 4. Comparable projections show, on the left, puckered hexagons of R (centered by Ni (orange) at alternating depths) that are condensed along the view as well as vertically via shared vertices to generate metal *sheets* separated by Te layers. This structure is known only for Y or Er with Z = Fe, Co, Ni.[18−20] On the other hand, $Sc_5Ni_2Te_2$ exhibits a different mode of condensation (right), *columns* of Ni-centered chains of octahedra condensed side-by-side along the view.[21] Lacking any more examples, a plausible ad hoc explanation of these differences arises from relative bond energy differences. The first motif with extended sheets yields the greater fraction of what are expected to be stronger R−R bonds than R−Ni bonds for Y, whereas the second version yields a larger fraction of Sc−Ni bonds, which are expected to be stronger for Sc and a late 3d interstitial than for Y−Ni.

Another naturally unanticipated result, $Sc_{14}Z_3Te_8$ (Z = Ru, Os; Figure 5), contains infinite chains of single trans-face-sharing $Sc_{8/2}(Z)$ *cubes* that alternate with pairs of similar *antiprisms* $[Sc_{8/2}(Z)]_2$, giving a net chain formula of $Sc_{12}Z_3$ (blue and green). These are, in turn, interbridged by shared $ScTe_6$ units, as shown.[22] It is particularly remarkable that the *same* metal chain construction is also found in $Sc_{12}Ir_3Br_{16}$, with the differences in the Sc and Te vs Br contents in the empirical formulas arising from different modes of bridging between the same metal chains.[23] The latter has 79 valence electrons, compared with 82 in the former.

A much more condensed result is found in the isotypic $R_{17}Ru_6Te_3$ phases (R = Er, Dy), which exhibit remarkably high metal contents, 88 atom % R + Ru.[24,25] The detailed construction shown in the projection in Figure 6 is rather complex, but close inspection will show that it consists mainly of chains of trigonal prisms of Er (blue) centered by Ru (black) that share basal faces, again viewed in the projection. The principal lateral condensation between the trigonal prisms means that their rectangular (side) faces are additionally tricapped by three Er atoms shared with their neighbors (see the side view below). Other motifs appear in lesser amounts. Again, tunnels are generated through the structures to accommodate Te (red) atoms and also in tricapped trigonal prisms of R. The stabilities of the most unusual phases among the heavier R group seem to parallel those of novel Sc and Y telluride products described earlier, evidently because of better R−Z mixing.[25]

A useful theoretical perspective from these studies is a renewed recognition of the sometimes irregular relationships between R−R distances and their bond populations (such as those measured by energy-weighted −COHP data). In other words, distances alone may not distinguish well between the effects of complex atom packing (size) restrictions and the less evident electronic effects from strong but delocalized interatomic bonding and high coordination numbers in many of these structures. Figure 7 shows two results from LMTO-ASA calculations on the metal-rich $Y_7Te_2$ shown in Figure 2b.[15] On the left, the density of states (DOSs) as a function of decreasing binding energies (left to right) are broken down according to atom and important orbital types by means of shading styles. (The plots are stacked so that visible areas are correctly weighted.) A pseudogap near −2.5 eV basically separates the DOS distributions into a valence band (left) with major Te 5p (singly hatched) and smaller Y contributions (black) from (right) a Y-dominated conduction band (filled to the dotted line at $E_F$) that is principally of Y 4d (cross-hatched) (and 5s) origins with negligible Te components. (Thus, the compound is in this sense polar and a bit

(19) Maggard, P. A.; Corbett, J. D. *Inorg. Chem.* **2004**, *43*, 2556.
(20) Magliocchi, C.; Meng, F.; Hughbanks, T. *J. Solid State Chem.* **2004**, *177*, 3896.
(21) Maggard, P. A.; Corbett, J. D. *Inorg. Chem.* **1999**, *38*, 1945.
(22) Chen, L.; Corbett, J. D. *J. Am. Chem. Soc.* **2003**, *125*, 1170.
(23) (a) Zimmermann, S.; Meyer, G. *Z. Kristallogr.* **2007**, *Suppl. 25*, 8-07. (b) Zimmermann, S. A. B. Dissertation, University of Cologne, Cologne, Germany, **2008**.
(24) Mehta, A.; Corbett, J. D. *J. Solid State Chem.* **2008**, *181*, 871.
(25) Herzmann, N.; Gupta, S.; Corbett, J. D. *Z. Anorg. Allg. Chem.* **2009**, *635*, 848.

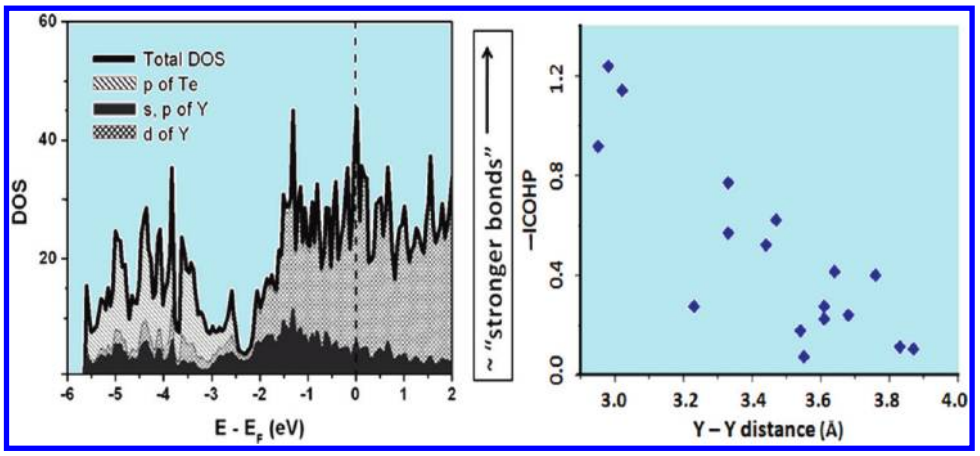


**Figure 7.** Some bonding lessons illustrated by the results of LMTO calculations on $Y_7Te_2$ (structure in Figure 2b). Left panel: DOSs (densities of band states) as a function of the energy that are filled by electrons up to $E_F = 0$. The shading scheme shows the significant separation of bonding states into, first, mixed Te 5p (single hatch) and Y 5s,p (black) (and a little 4d) states in a valence band for Y−Te bonding up to a clear pseudogap near −2.7 eV and, thereabove, a primarily Y−Y-based conduction band, mainly Y 4d (cross-hatched). Right panel: Comparison of −ICOHP data (∼relative Hamilton overlap populations) for different Y−Y bonds as a function of their individual distances that demonstrate some appreciable disparities between the two quantities and hence in the bonding (see the text).

"saltlike".) The plot on the right carries the punch-line, that there are appreciable contrasts between Y−Y distances and their corresponding −ICOHP values (the integrands of −COHP data up to $E_F$) for each bond, with the latter being good measures of relative (energy-weighted) bond overlap populations. Higher points in the distribution represent the stronger bonds (higher populations, relative to distance), whereas smaller −ICOHP values reflect lower populations and qualitatively lower bond strengths for those distances. The particular locations of the atoms involved in the latter situations afford very useful information about the bonding; the smaller relative−ICOHP values are always associated with Y atoms that have a larger number of Te neighbors. This arises because mixing (bonding) between Te 5p and Y 4d and 5s states on neighboring atoms decreases the energy of the lower-lying filled Te 5p states and correspondingly raises the d orbital energies on those Y. Of course, interior Y atoms with no Te neighbors are relatively unaffected. Thus, R−R bond lengths between those R with the greater number of Te neighbors are characteristically greater than those between R atoms that are mostly or entirely bound in active-metal-rich regions. (A comparable effect was noted and analyzed in $Sc_9Te_2$).[26] Under other conditions, one can easily imagine how distances between some atoms may be determined more by size in close-packed regions than by bond formation, sometimes referred to as "matrix effects". *"A distance does not a bond make"* and, perhaps, not a good approximation to its strength either.

## IV. Polyanionic Phases with Active Metals. Electron-Poorer Extensions of Zintl Phases and Beyond

Traditional Zintl phases[8] are the products of the reduction of post-transition metalloids and nonmetals by alkali metals, magnesium, and so forth, first identified at a time when the earliest structures of alloys and intermetallics were being analyzed and the concepts of bonding were very rudimentary. Parallels between their structure types and those of conventional salts were emphasized by Zintl. An important development was the later recognition by Klemm and Busmann[27] that the anion substructures obtained were often isosteric with those of the following elements and presumably isoelectronic with them as well. Thus, MgGa, LiGe, and $CaSi_2$ were all found to contain puckered sheets of three-bonded main-group elements that were reminiscent of (and isoelectronic with) those in hexagonal As, i.e., $(Tr^{-2}) \equiv (Tt^{-}) \equiv (Pn^{0})$ (except that the former structures were also stuffed with cations of the active metals). The area has come a long way since then, with a great many polyanion structures identified, both simple and complex. The most pertinent feature is that substantially all of the anion structural components can be understood in terms of classical valence bonding (octet rule) situations. Zintl also concluded that the left-hand boundary for p elements that yielded saltlike structure types (with Mg) lay between the group 14 (tetrel) and group 13 elements (triels in our nomenclature). However, our earliest studies of the reduction products of the latter triels with alkali metals showed that suitable (more modern) bonding rules had in effect already been recognized (first by Wade) for equivalent electron-deficient covalent bonding situations in the polyboranes ($B_nH_n^{2-}$, $5 \le n \le 12$) and related species.[28]

Many homoatomic as well as heteroatomic or centered examples of triel cluster anions have been subsequently identified (and reviewed),[29] mainly as alkali-metal salts. Three of the simpler but relatively unusual examples are shown in Figure 8. The $Tl_{13}^{11-}$ anion in $Na_3K_8Tl_{13}$ (a) fits easily into Wade's precepts through the centering of $Tl^{3+}$ in the corresponding closo-deltahedral $Tl_{12}^{14-}$ ($2n + 2$ skeletal electrons), the process of which brings no more valence electrons or new representations.[30] (Such a large cluster of a heavy element is presumably stabilized by the Tl "prop" too). The second, $In_{10}Zn^{8-}$ (b) in $K_8In_{10}Zn$, can be derived through centering of the analogous ideal $In_{10}^{12}(D_{4d}, 2n + 2)^{-}$ with $Zn^{2+}$, but the actual result has only $2n$ skeletal electrons instead.[31] Leaving a single highest occupied molecular orbital (HOMO) level empty in a distorted cluster is not

(26) Maggard, P. A.; Corbett, J. D. *J. Am. Chem. Soc.* **2000**, *122*, 838.
(27) Klemm, W.; Busmann, E. *Z. Anorg. Allg. Chem.* **1963**, *319*, 297.
(28) Corbett, J. D. In *Chemistry, Structure and Bonding of Zintl Phases and Ions*; Kauzlarich, S., Ed.; VCH Publishers: New York, 1996; Chapter 3, p 139.
(29) Corbett, J. D. *Angew. Chem., Int. Ed.* **2000**, *39*, 670.
(30) Dong, Z.-C; Corbett, J. D. *J. Am. Chem. Soc.* **1995**, *117*, 6447.
(31) Sevov, S. C.; Corbett, J. D. *Inorg. Chem.* **1993**, *32*, 1059.

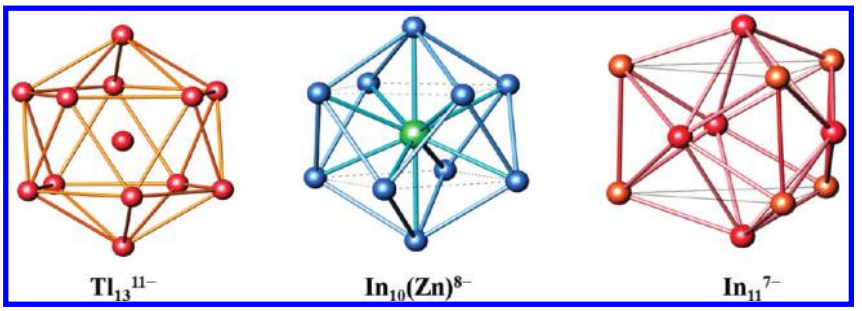


**Figure 8.** Three novel triel cluster anions isolated in the presence of relatively large amounts of alkali-metal counterions: $Tl_{13}^{11-}$, $In_{10}(Zn)^{8-}$, and $In_{11}^{7-}$. These show increasing electron deficiencies relative to Wade's rule values for closed-shell, delocalized cluster bonding (see the text for details).

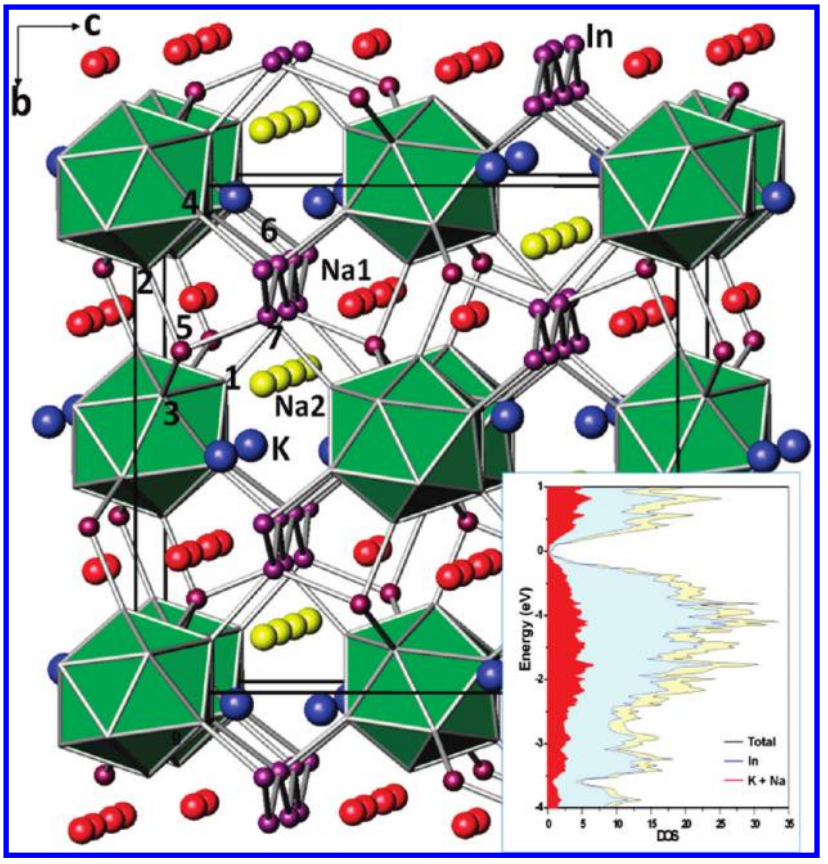


**Figure 9.** 3D network in $Na_3KIn_9$: $In_{12}$ icosahedra (green), In6,7 atoms in separate zigzag chains and isolated In5 atoms (dark red-purple), and Na and K cations (red and yellow). Classical analysis of the bonding suggests an ideal closed-shell configuration and semiconduction, but the phase is poorly metallic, in part, because of Na orbital contributions to the bonding shown in the insert (see the text for more details).

uncommon in this region; the electron affinities of the triels are certainly lower than those for the later elements, and the overall structural packing can be important, as follows. The third, $Tl_{11}^{7-}$, represented a new cluster configuration at the time, a *pentacapped* trigonal prism that exists only as a substantially electron-poorer ion with $2n - 4$ skeletal electrons.[32] (The latter can be easily explained by distortions for this particular symmetry). Yet another important variation in the stability of some solid-state structures appears in this case as well; the result is simply more stable (better packed) in its characteristic trigonal structure in the presence of one *extra* alkali-metal cation (plus an electron in a presumed conduction band), that is, as $(K^+)_8(In_{11}^{7-})(e^-)$ in a simplistic representation, loosely an "electron-rich Zintl phase". (The theoretical details of bonding in this have recently been examined in detail by Canadell and co-workers.[33]) On the other hand, the energetics that so often lead to Zintl (valence) phase formulations are sufficiently dominant that discoveries that "don't quite add up" are frequently examined with suspicion regarding possibly missing or misassigned atoms, with hydrides being great examples, viz., $Ba_5Ga_6H_2$.[34]

Many other types of triel phases exist with relatively lower proportions of active metal cations (and electrons), and their condensations into extended layers, networks, and so forth are natural results, some with quite complex motifs. Two

(32) Sevov, S. C.; Corbett, J. D. *Inorg. Chem.* **1991**, *30*, 4875.

(33) Cobián, M.; Alemany, P.; García, A.; Canadell, E. *Inorg. Chem.* **2009**, *48*, ASAP.

(34) Huang, B.; Corbett, J. D. *Inorg. Chem.* **1998**, *37*, 1892.

additional and important characteristics of the solid-state stability come into play on occasion: (1) long-range electronic bonding effects that pertain to infinite structures and (2) major influences that particularly favorable packing arrangements can have in certain structures. An example of the latter was just noted for the unexpected $K_8In_{11}$ and more follow. The use of alternate-sized or mixed cations has been well demonstrated to be a good way to gain new compounds and clusters via altered packing arrangements.[29]

**A. Metallic Properties.** Understanding the electronic characteristics of the face-centered $Na_6K_2(In_{12})In_6$ network structure illustrated in Figure 9 is complicated by more subtle electronic effects that may be important in the extended solid-state systems.[35] The $In_{12}$ icosahedra (green) are exobonded at all vertices to one of six separate In atoms (smaller red/purple spheres). Conversely, the latter six In are all 4-bonded, either to like In atoms in zigzag chains or to neighboring icosahedra or both (not all are easily seen here), and this makes them simple $In^-$ in oxidation states, isoelectronic with Sn. Red, yellow, and blue spheres mark Na1, Na2, and K positions. The assumption of complete charge transfer from the eight cations would exactly balance the needs of the ideal components $In_{12}^{2-}$ and $6In^-$. (The predicted excess of 14 electrons for an isolated icosahedral cluster $In_{12}^{14-}$ is reduced to $In_{12}^{2-}$ here, one for each cluster vertex that is exobonded to another In, nominally via oxidation of an $s^2$ pair). Thus, the compound is structurally closed shell, $(A^+)_8In_{12}^{2-}(In^-)_6$, and, as first thought, would seem to be a classical (semiconducting) Zintl phase. However, this simple interpretation is incorrect; the phase's resistivity is $\sim 49.5\,\mu\Omega$ cm at $\sim 295$ K, with a temperature coefficient of 0.46% $K^{-1}$, and its magnetism is close to that of typical Pauli-like (conduction electron) paramagnets ($\sim -3.8 \times 10^{-4}$ emu/mol). In other words, the phase is metallic, which requires the presence of some open states at the highest bound level (the Fermi energy, $E_F$). (Such effects are not unusual, particularly when we push on the boundaries of classical behavior in extended structures, but not very many "structural Zintl phases" have been checked regarding their actual conduction properties.[28]) In this case, only a pseudogap is calculated (via LMTO methods) at $E_F$ (see the inset in Figure 9); i.e., the behavior comes "close" to that of a semiconductor, but upon magnification the DOS is seen to not go to zero. The details of how and why open states occur here are too complex for this article, but indications of this behavior are found: first, Na states actually make substantial contributions to the calculated DOS over a wide range below $E_F$ (the red area in the inset relative to the total DOSs), contrary to the ideal model, and, second, several computed, mainly In-based, energy bands cross $E_F$ in all directions (in reciprocal space, not shown), giving the necessary open electronic states for 3D conduction. The extra components, the In6,7 atoms in the zigzag chain together with the separate In5 atoms (larger red-purple spheres), are largely responsible for these effects.

In fact, cations are generally not as innocent insofar as bonding is concerned as first thought, particularly with the less electronegative triel polyanions in these phases.

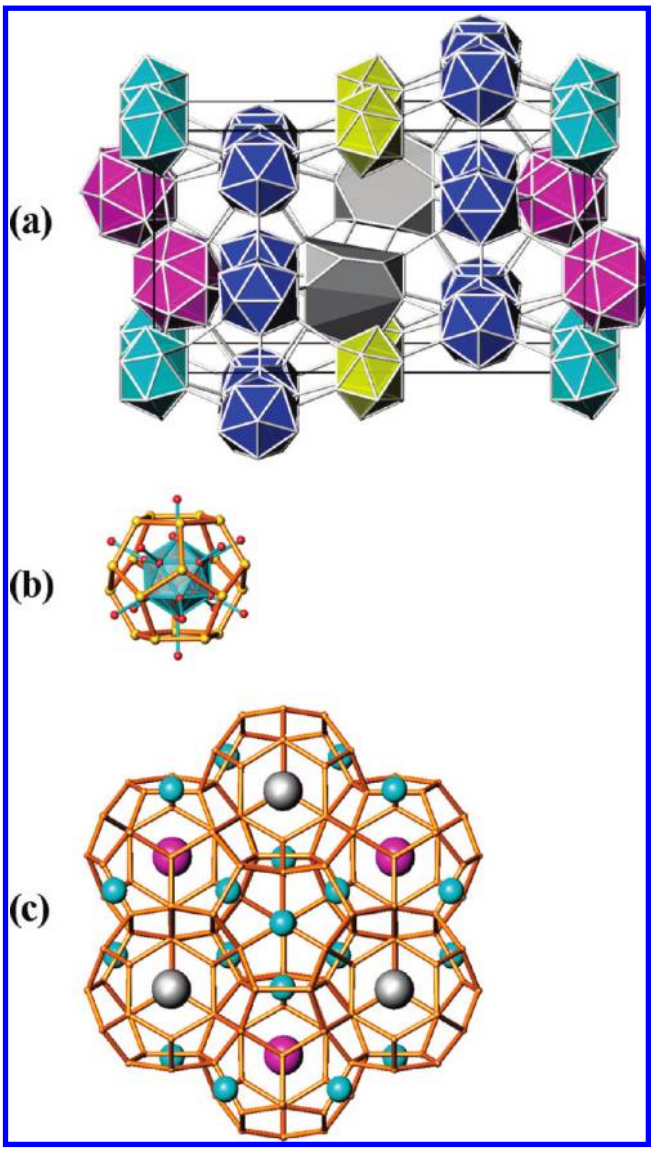


**Figure 10.** Three perspectives of the clathrate II type structure of $K_{39}In_{80}$. (a) Projection of the interbonded polyanionic clusters in the unit cell in which turquoise, blue, and yellow groups represent different $In_{12}$ icosahedra, the gray units are $In_{15}$ spacers, and the red polyhedra are $In_{17}$ clusters. (b) Detail of a single $K_{20}@In_{12}$ building block. (c) Overall framework representation in which K atoms lie at the intersections of light-brown framework lines and the turquoise, gray, and red spheres mark the locations of the respective $In_{12}$, $In_{15}$, and $In_{17}$ units within cation polyhedra.

This is especially so with Na,[36] whereas Li is not a significant component of Zintl phases but rather often introduces other novel chemistry (below). Participation of the higher d states on the alkaline-earth metals Ca−Ba is often substantial too,[37] as will be seen. Of course, these effects are still greater with trivalent cations, the rare-earth metals for example. We will return to these points.

**B. Long-Range Structural Organization: the Big Pictures.** Strong bonding in the polar intermetallic "salts" can lead not only to novel structural motifs but also to striking examples of longer range structural effects and complex packing. The progression to higher coordination numbers with the loss of directional bonding in polar

(35) Li, B.; Corbett, J. D. *Inorg. Chem.* **2006**, *45*, 2960.
(36) Li, B.; Corbett, J. D. *Inorg. Chem.* **2005**, *44*, 6515.
(37) Li, B.; Mudring, A.-V.; Corbett, J. D. *Inorg. Chem.* **2003**, *42*, 6940.

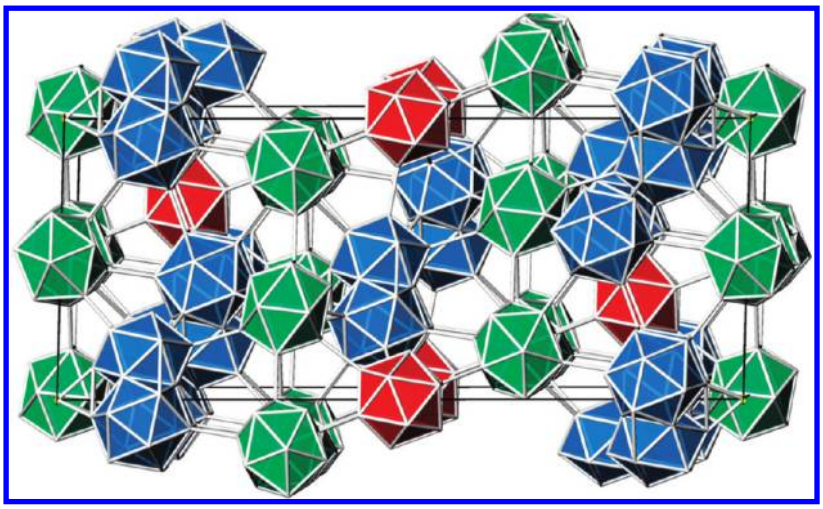

**Figure 11.** Interbonded cluster anions in the ideal (and unstable) rhombohedral $K_{34}In_{105}$, in which red and green units denote icosahedra of different symmetries and the blue units are condensed trimers of icosahedra. These types are encapsulated in $K_{20}$ and $K_{28}$ polyhedra, respectively (not shown), to generate another clathrate II structure (as in Figure 10). The ideal parent lattice is too electron-rich, and a complete vacancy-free lattice is obtained only if Li (or other suitable lower-valent atoms) are partially substituted on the least negative In sites (see the text).

intermetallics is part of this. Several novel examples follow.

(I) A supposedly simple binary example, $K_{39}In_{80}$, is a marvel of organization.[38] The smallest building blocks are $In_{12}$ icosahedra, but these occur in combination with lesser numbers of somewhat larger $In_{15}$ "spacers" and $In_{17}$ clusters, probably because of the particularly favorable packing of two basic units in what is called a *clathrate II* structure. Only the cluster parts of the unit cell contents are shown in Figure 10a, all of which are interbonded at all vertices. The rest of the structure can be well described in terms of a network of cationic $K_{20}$ and $K_{28}$ "clusters" (spatial arrangements) that very effectively encapsulate one of the two anionic clusters, $In_{12}$ (by $K_{20}$ in site C1) and $In_{15}$, $In_{17}$ (by $K_{28}$ in site C2). Figure 10b shows the first $In_{12}@K_{20}$ unit, including the exo bonds to other In clusters. The essence of the overall cation framework geometry is depicted in Figure 10c in a different way. The actual K atoms lie at all vertices, that is, points at which the yellow lines between them intersect. The locations of $In_{12}$, $In_{15}$, and $In_{17}$ clusters within the $K_{20}$ (in the center) or $K_{28}$ cages (around the outside) are now denoted by turquoise, gray, or red spheres, respectively ($P3$ symmetry).[38] The cage proportions in a clathrate II phase are $[A_{20}@C1]_2$:$[A_{28}@C2]$, and two such units are in the unit cell. The clathrate hydrates are perhaps most widely known, e.g., $(H_2S)_{16}(CCl_4)_8(H_2O)_{136}$. About a dozen examples of type II clathrates have been identified among In cluster compounds alone.

(II) Another magnificent structural and bonding example occurs in the neighborhood of the related rhombohedral lattice composition $A_{34}In_{105}$, A = K or mixed Na and K. For simplicity, only the anion lattice is shown in Figure 11.[39] This consists of nominal icosahedra with two different symmetries, A ($2/m$, green) and B ($3m$, red), and a trimer of icosahedra condensed around a 3-fold axis (C, blue), and all of these are again directly interconnected at all vertices through *exo*-In−In bonds. All are again enclosed in $A_{20}$ (A, B) or $A_{28}$ (C) cation cages in a space-filling clathrate II arrangement. The remarkable properties here are the electronic and chemical factors as they affect the stability. Problems were first manifested in the refined stoichiometries of both the nominal binary "$K_{34}In_{105}$" and its K−Na mixed cation version. For example, the latter gave, at best, a troubled refinement that could be expressed with some confidence as $K_{14}Na_{20}In_{96.30}\square_{8.70}$ only after an extensive analysis of the troubles following further reactions (□ represents partial vacancies on certain In sites in the A and C cluster types). In other words, ideal Na−K−In or K−In compositions with full site occupancies of the 105 In network sites could not be obtained. The vital clue came from other attempts to prepare cationic Li derivatives, because these instead yielded the same structure but with Li substituted on only those In positions in A and C that were otherwise troubled by fractional occupancy, not at K, Na, or other (possible) positions! Such products yielded refinements of $K_{34}In_{92.30}Li_{12.70}$ and $K_{14}Na_{20}In_{91.82}Li_{13.18}$ with full occupation of all 105 lattice sites. (Naturally, these mixed site refinements had to be buttressed not only by the high yields of single-phase products from reactions loaded with the refined compositions but also by direct Li analyses of single crystals).

An interpretation of these features started with the postulate that the full $A_{34}In_{105}$ lattice must be too electron-rich. This is easily verified by simple extended Hückel calculations for the complete lattice, which put $E_F$ well above a pseudogap in a region of antibonding In−In states. In fact, the valence electron counts per cell from the refinements of the first incomplete K−Na−In lattice and of the two Li products above are quite close, 970.8, 967.9, and 968.7, particularly when it is recalled that the first corresponds to the upper limit obtained in the presence of excess In, not the optimal amount. The Li substitutions serve to lower the total electron count, and these occur at those In sites in the hypothetical ideal lattice that have the smaller calculated site potentials.[40]

(38) Li, B.; Corbett, J. D. *Inorg. Chem.* **2003**, *42*, 8768.
(39) Li, B.; Corbett, J. D. *J. Am. Chem. Soc.* **2005**, *127*, 926.
(40) Miller, G. J.; Lee, C.-S.; Choe, W. In *Inorganic Chemistry Highlights*; Meyer, G., Naumann, D., Wesemann, L., Eds.; Wiley-VCH: Weinheim, Germany, 2002; pp 21−53.

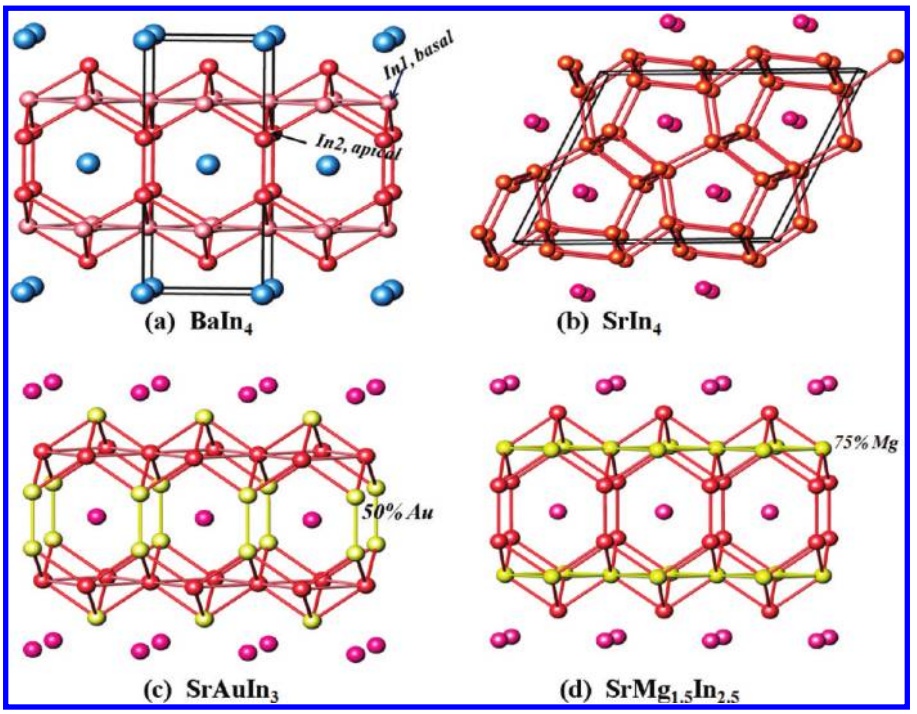


**Figure 12.** Size effects among tetragonal $BaIn_4$-type structures (a) as a function of the comparative sizes of both cations (Ba, blue, or the smaller Sr, red, in parts b−d) and of the interconnected In-type network atoms. The latter are of two types, red and pink in part a and, additionally, yellow for Au or Mg substituents in the (c) isostructural $SrAuIn_3$ and (d) $SrMg_{1.5}In_{2.5}$, respectively (see the text for details).

Both similar sizes and electronegativities ($X$) are important for the In−Li mixing, with the latter being 3.1 and 3.0 on the Mulliken scale.[41] (The absence of Na on In sites must result mainly because of size differences). These observations can have a further importance in that they introduce rational means to *tune* the electronics and properties of intermetallic (and presumably other) compounds. Thus, alternate substitutions of In by Mg or Zn ($X$ = 3.8 and 4.4, respectively) in the same structure are not so surprising, although other factors are certainly also involved. Simple theoretical calculations do not allow for the fact that these phases are probably all poor metals too.

**C. $BaAl_4$-Type Lattices.** Critical size and packing effects can be readily demonstrated in terms of stability, or not, of the very common $BaAl_4$-type host lattice, which is shown in Figure 12a for the specific example of $BaIn_4$. This body-centered structure type ($I4/mmm$) is well-known for the evident tightness of the optimal packing within and between the 3D tetragonal network cages of In (red and pink) and the centered Ba atoms (blue), all of which lie on vertical 4-fold axes through the condensed In cages.[42] Each cage unit consists of 8 + 4 In neighbors, four (*apical*) $In_2$ dimers (red) on the side edges around each Ba neighbor, and two pairs of *basal* (pink) In atoms above and below. The last in themselves are better defined in terms of relatively open horizontal square sheets of (pink) In atoms that are additionally capped on alternate sides by the closely bound apical In atoms (red). The hexagonal rings that define the faces of the cages about Ba are a useful key because the structure collapses into a more complex monoclinic array with only five-membered In rings when Ba is replaced by the smaller Sr in $SrIn_4$ (Figure 12b).[43] One can imagine that Sr would otherwise "rattle" in the oversized In cages, which would not optimize the strong bonding interactions between the two. However, reversion of a $SrIn_4$-type to a $BaIn_4$-type host lattice can be gained via three different substitutions of other atoms into the In network, all of which shrink the In lattice to better fit Sr. These are more or less geometric adjustments, although some electronic "tuning" may occur as well. (Substitutions in other $BaAl_4$ examples have shown that the basal sites are more suitable for more electropositive or larger atoms and the apical for more electronegative (and/or smaller) atoms when other factors are less important).[42] Thus, the structure returns to the tetragonal parent type upon substitution of 50% of the smaller and more electronegative Au atom into the apical In positions in part c, $SrAuIn_3$,[44] because the In−Au bonds are shorter than the former In−In (see more in section VI). Correspondingly, random substitution of the slightly smaller but more electropositive Mg for 75% of In in the basal (pink) layers shrinks the lattice laterally enough for $SrMg_{1.5}In_{2.5}$ to form in the tetragonal structure (with some adjustments of other free parameters), as marked by the yellow layer in Figure 12d. Finally, substitution of the smaller and more electronegative Zn into the apical positions also yields the isotypic $SrZnIn_3$.[45]

**D. Another Close Fit: $Na_4K_6Tl_{13}$.** Explorations for more varieties of clusters along with, as always, some serendipity led to the discovery of several derivatives of centered and nominally icosahedral $Tl_{12}M$ and $Tl_{13}$ cluster anions as alkali-metal salts. The packing in these and

(41) Pearson, R. G. *Inorg. Chem.* **1988**, *27*, 736.
(42) Häussermann, U.; Amerioun, S.; Eriksson, L.; Lee, C.-S.; Miller, G. J. *J. Am. Chem. Soc.* **2002**, *124*, 4371.
(43) Seo, D.-K.; Corbett, J. D. *J. Am. Chem. Soc.* **2000**, *122*, 9621.
(44) Liu, S.; Corbett, J. D. *Inorg. Chem.* **2004**, *43*, 4988.
(45) Li, B.; Corbett, J. D. *Inorg. Chem.* **2007**, *45*, 8812.

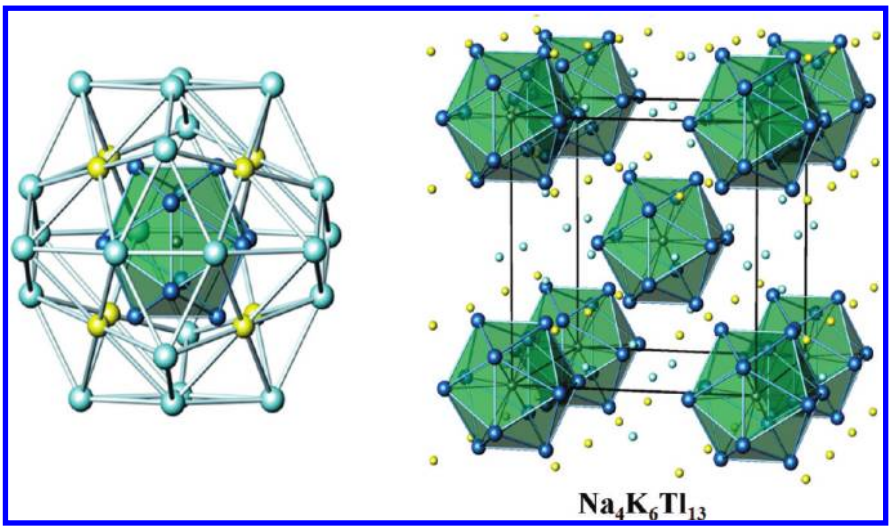


**Figure 13.** Details of the cubic $Na_4K_8Tl_{13}$ structure as a starting point to new AC and QC phases. Left: Details of the close Na (yellow) and K (light blue) encapsulation of the icosahedral $Tl@Tl_{12}$ cluster (green). Right: Body-centered-cubic unit cell of the same phase.

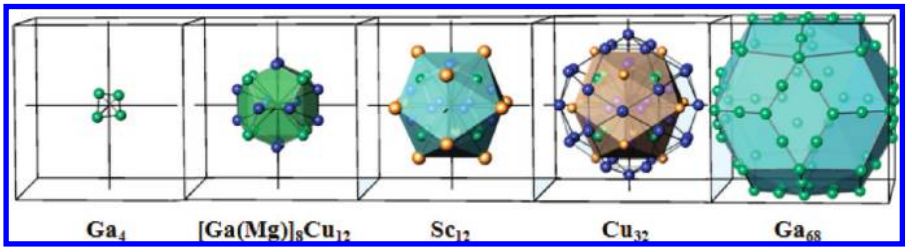


**Figure 14.** Multiply-endohedral shells that constitute the 1/1 (Tsai-type icosahedral) AC $Sc_{14.2}Mg_{0.2}Cu_{49.7}Ga_{34.3}$, with the atom contents on each shell listed. The distributions of atoms of different electronegativities or acidities among the shells are intrinsic in this and other such structures.

hence their stabilities are strongly governed by the cationic partners, in both size and number. By far the most remarkable is $Na_4A_6Tl_{13}$ (A = K−Cs), which is represented in Figure 13 both for the refined cluster (green) with its sheath of Na (yellow) and K (light blue) neighbors (left) and for the complete body-centered-cubic cell ($Im\bar{3}$, A = K) (right).[30] (Note that disorder among mixed cations in the solid-state compounds of this type has not been observed, even between those of the same charge type, meaning that the packing of the components in these structures must be very selective and any phase widths from cation mixing, very small.) In the present case, the Na atoms (yellow, left view) lie on (diagonal) 3-fold axes of the cubic cell and cap triangular faces on the icosahedra. In fact, the 32 atoms in the cation shell cap all 20 faces and bond exo at all 12 Tl vertices! This disposition throughout the extended solid means that the cations play very concerted roles in cementing the structure, with the Na atoms, for instance, bridging between faces on adjoining icosahedra (yellow, right). In addition, the 4−6−13 stoichiometry also means that an odd number of valence electrons are present in the cluster, and the compound is Curie−Weiss paramagnetic ($\Theta = -96$ K), with one hole in the cluster HOMO and also, incidentally, a poor metal ($\rho_{293} = 310\,\mu\Omega$ cm; $d\rho/dT = 0.29\%\ K^{-1}$). The structural packing represented in Figure 13, which fixes the stoichiometry, is clearly more important than that of a diamagnetic product. The related and nominally closed-shell anion in $Na_3K_8Tl_{13}$ ($R\bar{3}m$) has a comparable cation shell about each icosahedron but less distinctive packing in the overall lattice.[30] Some "tuning" chemistry also allows access to primitive ($P\bar{3}m$) derivatives of the former, with centered $Tl_6$ octahedra in the center instead, namely, $Na_{14}K_6(Tl_{12}M)(Tl_6)$ (M = Mg, Zn−Hg).[46] (An increase in the Na proportion in this phase evidently serves to "solvate" the smaller octahedron better.) This composition and structure later led us to a successful entrance into new materials in the field of quasicrystals (QCs) and, particularly, of their more conventional crystalline approximants (ACs), as follows.

## V. New AC Phases and Their Quasicrystalline Parents

QCs are relatively new and certainly unusual forms of crystalline matter in that they lack the traditional translational symmetry of normal crystalline materials that is the bedrock of conventional crystallography. Their complex quasiperiodicity means that their structures are presently unknown in detail. The name is not to imply that they are somehow poorly crystalline: QCs are well-crystallized judging from conventional powder X-ray diffraction, giving sharp lines and relatively easily recognized powder patterns, but higher dimensional crystallographic means are necessary to classify these. We will not pursue QC questions further; more chemical details and references are given elsewhere.[47]

Fortunately for chemists, QC materials evidently always have (crystallographically normal) AC neighbors that are evidently made up of very similar structural components, at

(46) Dong, Z.-C; Corbett, J. D. *Angew. Chem., Int. Ed. Engl.* **1996**, *35*, 1006.

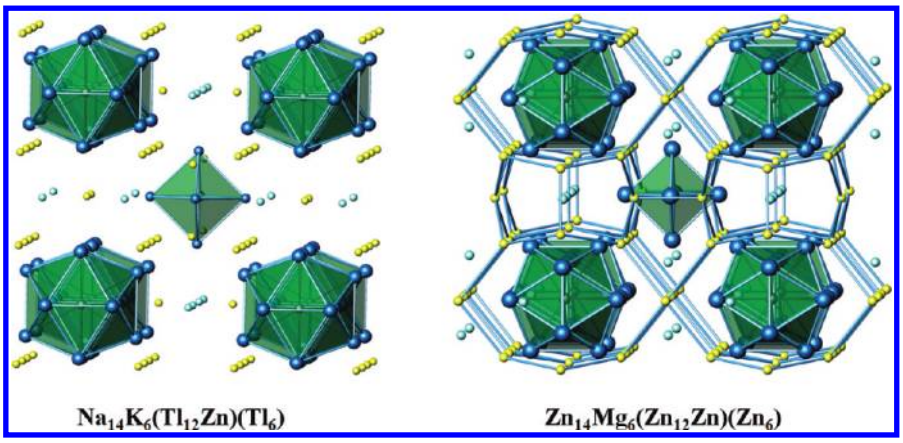


**Figure 15.** Concept of a synthetic route to new 1/1 and 2/1 ACs and QCs according to structural similarities. Left: Structure of a primitive cubic analogue of $Na_4K_8Tl_{13}$ (Figure 13), namely, $Na_{14}K_6(Tl_{12}Zn)Tl_6$, which is isostructural with $Mg_2Zn_{11}$ ($=Zn_{14}Mg_6(Zn_{13})Zn_6$), right. The $Zn_{14}$ (yellow) group on the right, the equivalent of $Na_{14}$, is shown as a network enmeshing the cluster groups. The reduced Mg−Zn polarity is important for better electron delocalization in the prospective AC/QC systems.

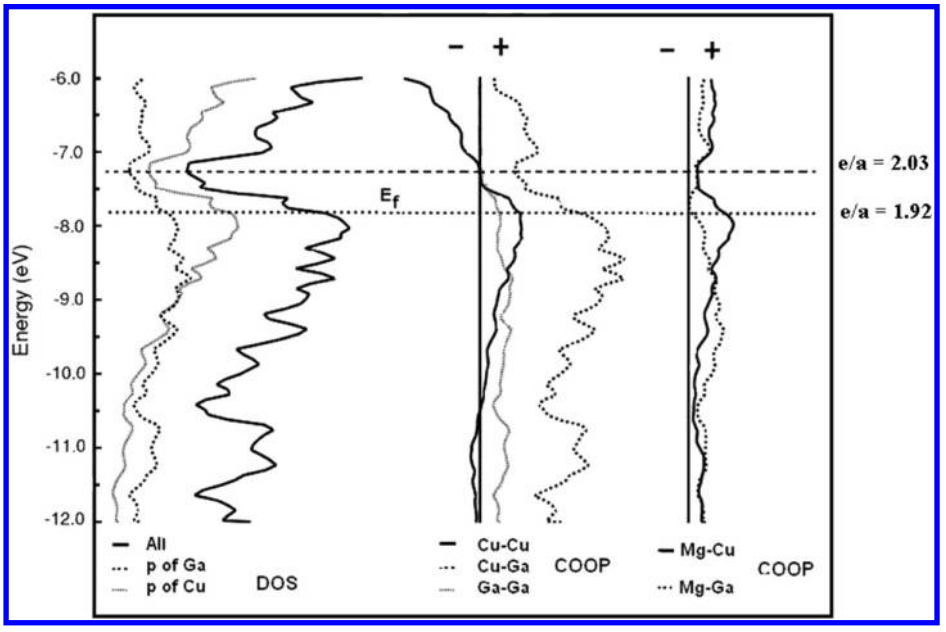


**Figure 16.** Results of an extended Hückel calculation on $Mg_2Cu_6Ga_5$ (e/a = 1.92), a $Mg_2Zn_{11}$ isotype, which shows a prominent pseudogap in DOS near e/a = 2.03 (left) and empty bonding states up to about that point according the COOP on the right.

least in the very few QC examples that are better understood.[48] Among QCs, those with 3D icosahedral symmetry (i-QCs) are most common, and among these, only the more common Tsai-type ACs [named after the discoverer of the remarkable binary QCs in the (Ca,Yb)−Cd systems] will be considered here. In terms of idealized components, an i-QC is said to be of Tsai type if its 1/1 cubic AC (in the icosahedral subgroup $Im\bar{3}$) contains the 66-atom, multiply-endohedral cluster sequence of, from the center out, a disordered tetrahedron (4 atoms), a pentagonal dodecahedron (20), an icosahedron (12), an icosidodecahedron (30), and an outermost triacontahedron (60) [plus, perhaps, additional decorations (atoms) on or near the last one]. Figure 14 shows this sequence for the cubic $Sc_3Mg_{0.2}Cu_{10.5}Ga_{7.25}$ with the refined compositions for each shell listed ($a$ = 13.5005 Å).[49]

(Strong bonding also occurs between these shells, but this is difficult to represent in the figure. Actually, a series of approximants, 1/1, 2/1, 3/2, ... (a Fibonacci series), describe the progression of an AC series toward the QC, although only the first two members are presently known from good X-ray diffraction refinements.) Several types of local defects are often observed, especially fractional or mixed site occupancies, as well as additional "decorations".

Our initial purpose in exploring these systems was to see whether solid-state cluster chemistry experiences could contribute to a field that had been dominated by researchers from other fields. These efforts started with modifications of likely precursors in attempts to fit these into typical AC structure classes as well as elemental substitutions to gain evidently favorable electronic regions, that is, electron/atom (e/a) counts of around 1.8−2.2 (averaged over all atoms and omitting filled $d^{10}$ shells). The novel example in Figure 13, $Na_4K_6Tl_{13}$, seemed apropos inasmuch as it contained evidently favorable icosahedra and occurred in the same $Im\bar{3}$

(47) Lin, Q.; Corbett, J. D. *Struct. Bonding* (*Berlin*) **2009**, *133*, 1.
(48) Takakura, H.; Pay Gómez, C.; Yamamoto, Y.; de Boissieu, M.; Tsai, A. P. *Nat. Mater.* **2007**, *6*, 58.
(49) Lin, Q.; Corbett, J. D. *J. Am. Chem. Soc.* **2005**, *127*, 12786.

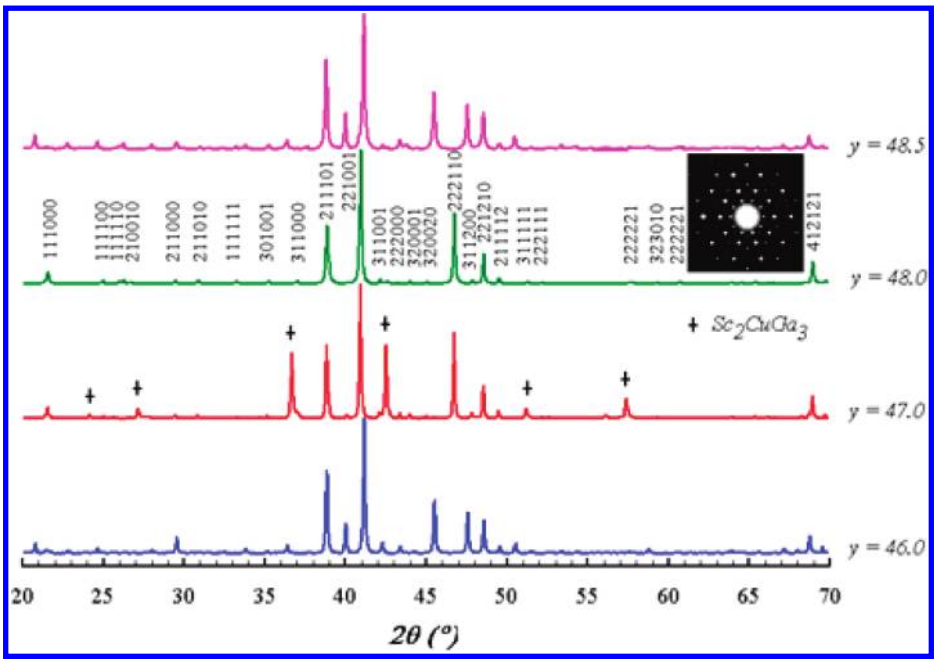


**Figure 17.** Guinier powder patterns that guided the final search of $Sc_{15}Mg_3Cu_yGa_{82-y}$ compositions, following the results shown in Figure 16. The substantially pure 1/1 product (e/a = ~2.01) appears at $y$ = 46.0 and 48.5 and the QC at $y$ = 48.0. The inset is the electron diffraction pattern for the QC along its 5-fold axis.

space group as was already known for Tsai-type 1/1 examples. However, according to known examples, it also seemed unlikely that the electropositive elements Na, K, etc., would participate well enough in the rather broad electronic delocalization that seems characteristic of ACs and QCs. Fortunately, Tl icosahedra centered by other elements in a primitive version ($Pm\bar{3}$) of the structure type gave us the key. As shown in Figure 15, $Na_{14}K_6(Tl_{12}M)Tl_6$ (left), with $Tl_6$ octahedra centering a simple cube of $Tl_{12}M$ icosahedra (M = Mg, Zn−Hg),[45] is also isostructural with $Mg_2Zn_{11}$,[50] which in terms of parallel functional groups is constituted $Zn_{14}Mg_6(Zn_{12})Zn_6$ (right), in which the first two groups take the cation positions in the former. (The $Zn_{14}$ "unit" is now shown as a blue network spread over the former Na positions). An important attribute here is that the elements Mg and Zn are much more similar in electronegativity and bond polarity than the Na and K cations in the former Tl "salt" and, accordingly, are much closer to what we sought. Structure types and their packing similarities appear rather important in many instances, and so we set out to "tune" all known or probable $Mg_2Zn_{11}$-type analogues through substitution of chemically and electronically similar elements in order to attain suitable e/a values in new ACs and, ultimately, new QCs. And this worked!

QCs are known to exhibit electronic pseudogaps at the Fermi level (the highest-filled energy bands) that are associated with special electronic stability effects at their compositions, and our presumption/hope was that the ACs might behave likewise (and they do!). Therefore, an e/a target was (naively) estimated from an electronic structure calculation on the first trial phase, $Mg_2Cu_6Ga_5$, a new $Mg_2Zn_{11}$ isotype with e/a = 1.92.[51] According to an extended Hückel calculation (Figure 16), incompletely filled bonding states for Cu−Cu, Cu−Ga, and Ga−Ga in the crystal orbital overlap

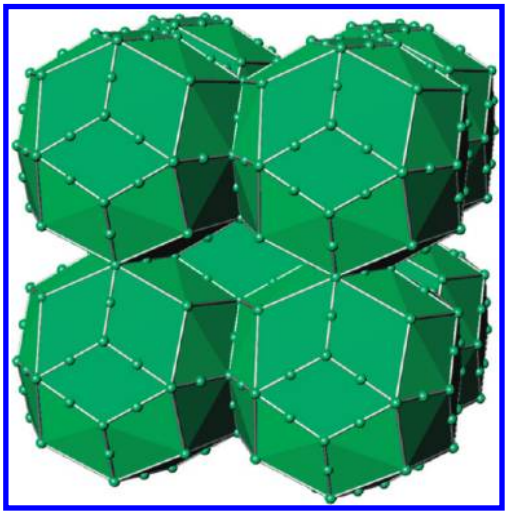

**Figure 18.** The extended body-centered-cubic unit cell of 1/1 Tsai-type ACs, with each polyhedral unit being a condensed array of the cluster types shown in Figure 14.

population (COOP) plots (right) lie just below a pseudogap in the DOS (left), suggesting that bonding in a composition nearer e/a ~ 2.03 could be better. Indeed, subsequent incremental additions of mainly Sc in place of Mg (followed by powder pattern checks) yielded the $Im\bar{3}$ pattern for the 1/1 AC at the (normalized) composition $Sc_{14.2}Mg_{0.2}Cu_{49.7}Ga_{34.3}$ (e/a = 2.01) and, subsequently, the QC at a nearby $Sc_{15}Mg_3Cu_{48}Ga_{34}$ composition (e/a = 2.01) (as identified by its proper 5-, 3-, and 2-fold rotational symmetries). The small Mg contents appear to be essential for stability. Figure 17 shows the powder pattern guidance achieved in the final stage of this search among $Sc_{15}Mg_3Cu_yGa_{82-y}$ compositions, namely, the essentially clean 1/1 IC pattern at $y$ = 46.0 and 48.5 and that of the QC at $y$ = 48.0. (Some nonstoichiometries, that is, from variable mixed or fractional atoms on some lattice sites, are not unusual in these phases.)

(50) Samson, S. *Acta Chem. Scand.* **1949**, *3*, 835.
(51) Lin, Q.; Corbett, J. D. *Inorg. Chem.* **2003**, *42*, 8762.

Similar explorations and AC/QC results have since been achieved in the Sc−Mg−Zn,[52] Ca−Au−In,[53] and −Ga,[54] −Sn, and −Ge[55] systems, with significant changes in the structural details among these nominally isotypic AC phases as well. The introduction of the Ca−Au pair of elements in the last four was the lucky result of an idea to replace Cd in the binary Ca−Cd AC and QC system by Au + In in order to achieve both better differentiation of the atoms (in size, site occupancies, and diffraction) and easier alteration of the electron counts. This occurred at about the same time that Au was discovered to play a very productive, virtually magic, role in generating new chemistry in many other triel systems (below). Imagination plays a valuable role in explorations, and certainly luck as well.

The multiply-endohedral shells of Tsai type in a 1/1 AC in Figure 14 (including the outermost triacontahedron) are characteristic. The 1/1 unit cell (Figure 18) consists of a partially condensed, body-centered-cubic array of the aggregate of these polyhedral units, and only changes within these shells appear to differentiate between this Tsai and another Bergman-type AC (QC) family. In other words, the geometric differences between these types appear to be short-ranged and contained entirely within the 1/1 building units. The same is true of the larger and more complex cells of the 2/1 ACs. A further significant feature of such complex structures is that the distributions of appreciably different atom types among these polyhedral shells are fixed by the AC structure type, the atoms involved, and, therefrom, the electronic structures. That is to say, the location of the more electropositive atoms, Sc in the third icosahedral shell in Figure 14 for example, is determined solely by the structure (and the elements), with these being the positions with the intrinsically lowest site potentials or valence electron populations in all isostructural Tsai-type examples. (The availability of d valence orbitals on these cations is evidently necessary too).[56] On the other hand, the more cationlike elements in the different Bergman-type 1/1 ACs, say Mg in the Mg−Al−Zn example, are found instead in the second and fifth (dodecahedral and triacontahedral) shells, respectively. The geometrically and chemically different first and fourth shell contents in the Tsai versus Bergman classes are the principal structural differences in the respective 1/1 and 2/1 ACs and, presumably, also in their QCs.[57] These regularities reflect complex structural and bonding effects in general, not just in these systems, and ones that are evidently intrinsic to the specific structures. Full icosahedral symmetry ($m-5-3$) cannot be replicated only by translational means, but the periodic AC structures observed, in fact, appear to be geometrically close to this symmetry limit.[47]

Our procedure of predicting e/a values for pseudogaps in new AC and even QC systems according to calculations on a neighboring phase, an $Mg_2Zn_{11}$ type or a lower AC for example, likely involves some luck (or sophistry) because we are applying the prediction across a phase boundary (structural change), and this property should not be so simply transferable. In fact, pseudogaps for many of the 1/1 and 2/1 AC products have very similar e/a values, or at least values that are close enough to each other that their neighbors can often be found through more or less simple compositional tuning (and powder pattern) experiments, as shown in Figure 17. *The structures themselves appear to signal the proximity of such electronic events*. In other words, even the $Mg_2Zn_{11}$ structure type in a subgroup of the AC symmetry has some information built into it about compositions with special electronic conditions. A good deal of serendipity is probably built into this process as well. Complex ternary and higher systems have, in general, been poorly explored regarding new phases and structures, and stumbling on these affords great openings to new chemistry. The remarkable $Ca_4Au_{10}In_3$ result (below) is a great example.

## VI. Intermetallic Magic with Gold

Although a great deal has been published regarding reduced Au compounds with positive oxidation states, Au's negative states have not been well studied beyond the classic $5d^{10}6s^2$ "pseudohalide" state in CsAu. However, clear hints of a broader chemistry originated first with Sinnen and Schuster[58] and then Zachwieja[59] regarding condensed $Au_7$ dimers of Au tetrahedra interbridged by $Tt_2$ units, and Zachwieja later described several unusual more condensed Au phases.[60,61] It has now become very clear that a good deal of new chemistry can be achieved among ternary or higher intermetallic compounds in which Au is reduced to (formal) negative oxidation states, at least for those with an alkali-metal (A) or alkaline-earth-metal (Ae) component. Evidently, strong bonds and diverse polyanionic bonding motifs are generated between Au and many of the post-transition metals and metalloids. For our part, this expansion came out of our efforts to extend Zintl phase ideas, but its breadth and impact have now evolved considerably.

At the present stage, the dominance of relativistic effects[62] for Au provides the most direct explanation for the plethora of new phases and structures. Although its sixth-period neighbors Pt and Hg, and maybe others, should also participate significantly, Au has so far been the most productive. In simple terms, this phenomenon leads to tighter binding of the outer 6s orbitals and, in parallel, relatively less binding of the 5d set and thus greater 6s−5d mixing, with the former, in particular, also decreasing the Au atom's effective radius and hence bond lengths. [Recall the structural contraction between $SrIn_4$ and $SrAuIn_3$ (Figure 12)]. These changes in fundamental parameters also lead to a marked enhancement of Au's Mulliken electronegativity (the average of the gaseous atom's electron affinity and first ionization energy),[44] putting the Au value (5.77 eV) in the neighborhood of those of P, Se, and Te. This suggests not only enhanced bond strengths between Au and later but distinctly less electronegative metalloids such as In, Tl, and Sn but also notably stronger bonding interactions between Au and some cations, Ca and K for example, relative to, say, those exhibited by reduced triel or tetrel elements.

(52) Lin, Q.; Corbett, J. D. *J. Am. Chem. Soc.* **2006**, *128*, 13268.
(53) Lin, Q.; Corbett, J. D. *J. Am. Chem. Soc.* **2007**, *129*, 6789.
(54) Lin, Q.; Corbett, J. D. *Inorg. Chem.* **2008**, *47*, 7651.
(55) Lin, Q.; Corbett, J. D. Unpublished research.
(56) Mizutani, U. In *The Science of Complex Alloy Phases*; Massalski, T. B., Turchi, P. E. A., Eds.; The Minerals, Metals & Materials Society: Warrendale, PA, 2005; p 1.
(57) Lin, Q.; Corbett, J. D. *Proc. Natl. Acad. Sci.* **2006**, *103*, 13589.
(58) Sinnen, H.-D.; Schuster, H.-U. *Z. Naturforsch.* **1981**, *36b*, 833.
(59) Zachwieja, U. *Z. Anorg. Allg. Chem.* **1998**, *624*, 1443.
(60) Zachwieja, U.; Wlodarski, J. *Z. Anorg. Allg. Chem.* **1998**, *624*, 1569.
(61) Müller, J.; Zachwieja, U. *Z. Anorg. Allg. Chem.* **2000**, *626*, 1867 and references cited therein.
(62) Pyykkö, P. *Angew. Chem., Int. Ed.* **2002**, *41*, 3573.

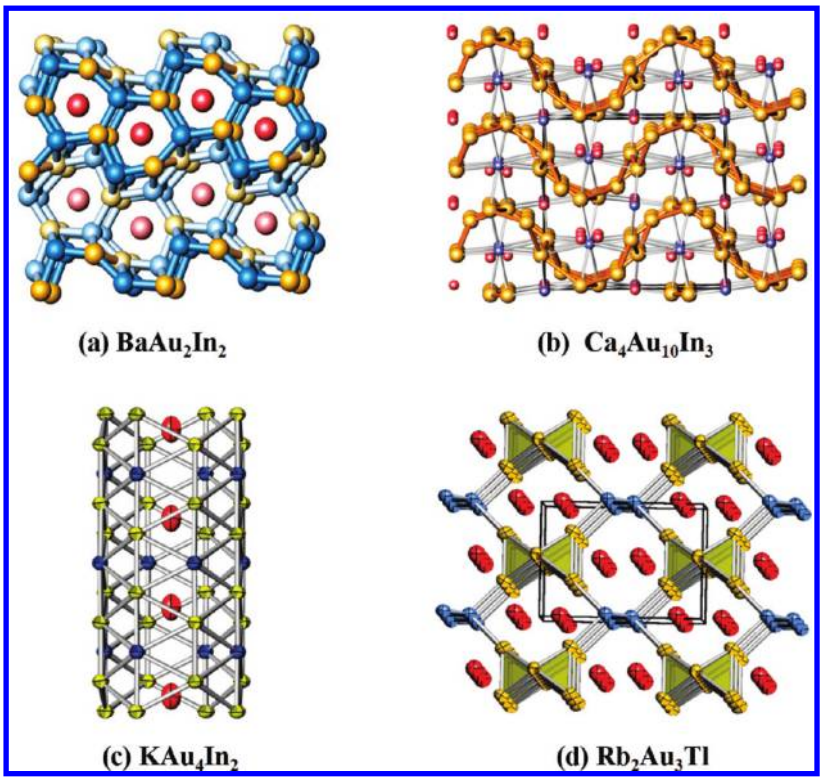


**Figure 19.** Four "magic Au" results: (a) Rather complex hexagonal prismatic encapsulation of Ba (red and pink) in a condensed Au−In network in $BaAu_2In_2$, giving an enhanced coordination number to the former and alternating Au−In bonds in the network. (b) Novel $Ca_4Au_{10}In_3$ discovered during explorations in the Ca−Au−In system, showing the infinitely wavy Au sheets in the projection. Red and blue spheres mark the isolated Ca and In positions, respectively. (c) $KAu_4In_2$, one of several tunnel structure types that occur in this ternary system. The structure extends laterally via Au and In atoms that are shared between tunnel walls. (d) Remarkable $Rb_2Au_3Tl$, one of a number of compounds that show aggregation of $Au_4$ tetrahedra, with these usually sharing vertices with other $Au_4$ to generate extended Au chains or sheets. Numerous close cation−Au interactions also appear to be significant in the overall stability of this group of remarkable phases.

Four structural results depicted in Figure 19 briefly illustrate these features: (a) $BaAu_2In_2$; (2) $Ca_4Au_{10}In_3$; (c) $KAu_4In_2$; (d) $Rb_2Au_3Tl$. These are uniformly composed of an active A or Ae metal, a substantial proportion of Au, and In or Tl, with the principal variations arising from changes in either the cation type or the relative proportions of the three components. These brief looks are principally intended to impart some qualitative feelings about some unusual features and differences in recent discoveries.

(a) Characteristic of most members of an appreciable Ae−Au−Tr family, $BaAu_2In_2$ exhibits a complex 3D condensation of hexagonal prisms of Au−In that tightly encapsulate the Ae (=Ca−Ba) cations.[59] One driving force appears to be to give each Ae the largest number of network Au and Tl atoms as possible, within packing limitations. Note the alteration of Au and In in the bonding, presumably because of a large bond polarity. The simple hexagonal prisms are logically augmented by up to six In and Au members of adjoining (but displaced) prisms that are coplanar with Ba and thus cap side faces of the hexagonal prisms. A further relatively complex 3D condensation of the capped prisms reflects particularly the low proportion of cations to network atoms, giving zigzag chains of like prisms that share prismatic edges (horizontal, darker blue/gold). These are paralleled by the same type of lighter-colored chains that are displaced by half of the projection repeat so as to provide augmentation of Ba coordination in the darker chain, and vice versa. Finally, the 3D solid comes about through infinite sharing of the basal faces of the hexagonal prisms along the view. The variety of structures of this character that are possible among different systems and elements seems quite large.

(b) The amazing $Ca_4Au_{10}In_3$ (Figure 19b) was stumbled onto while exploring phase space for the neighboring Ca−Au−In ACs and QCs.[64] The presence of over 50 atom % Au is a clear novelty, as in the following examples as well. The wavy sheets of Au seen in the profile are interbonded by Ca (red) and In (blue), with rather different functions. The phase is isostructural with $Zr_7Ni_{10}$, but the transformation from this to $Ca_4Au_{10}In_3$ conceptually involves some clearly complex atom exchanges (transmutations) and electronic processes. This discovery affords great support for the value of exploratory syntheses.

(c) Relatively larger amounts of alkali-metal cations with triels alone generate small polyanions and related networks of borane-related (Wade's rule) species, as in Figure 8, some even binding relatively small amounts of Au. However, substantial decreases in the cation content and increases in the Au−Tr proportion to greater than 1:1 yield distinctive tunnel structures, such as for $KAu_4In_2$ in Figure 19c.[65] (These are further condensed laterally via shared wall atoms into polyanionic nets of parallel tunnels). Three other compositions in the same system also give closely related structures. The cations centered in the tunnels are more or less localized, depending on variations in the inner wall structures. Several

(63) Dai, J.-C.; Corbett, J. D. *Inorg. Chem.* **2007**, *46*, 4592.
(64) Lin, Q.; Corbett, J. D. *Inorg. Chem.* **2007**, *46*, 8722.
(65) Li, B.; Corbett, J. D. *J. Am. Chem. Soc.* **2006**, *128*, 12392.

of these are remarkably (kinetically) inert as bulk materials, some to water and even 12 M HCl at room temperature.[66,68]

(d) Other surprises are still being found. Further increases in alkali-metal and gold proportions in the presence of In or Tl yield yet other remarkable results that are particularly distinctive because of the presence of both (1) Au *tetrahedra* that share vertices to generate Au sheets or chains and (2) multiple cation−Au interactions that contribute significantly to the overall bonding of the solids.[67] One of the simpler examples is shown in Figure 19d for $Rb_2Au_3Tl$, in which chains of $Au_4$ are generated through the sharing of half of their vertices, alternately left and right in the projection. The other two vertices on each tetrahedron are bonded to interlinking zigzag chains of four-bonded Tl (blue). Another example of this type exhibits greater condensation into puckered sheets of tetrahedra that share three vertices, $K_3Au_5M$ (M = In, Tl,[66] Pb[60]). The numerous cation−Au contacts (∼10/cation) in these two types also appear to be particularly significant in their stabilities inasmuch as these contribute significant fractions of the total −ICOHP (≈bond population) sums per cell. Although the individual A−Au values are rather small, 10−15% of those for Au−Tr, the former are 8−12 times more numerous. This segregation of Au and Tr bonding in the presence of low Tr but high A content is in striking contrast to the dominance of polar Au−Tr bonding in other instances (Figure 19a,c for instance).

## VII. Generalities and Afterthoughts

Much of this new chemistry can, in hindsight, be formally organized in terms of charged networks of mixed metals that are paired with more or less simple anions or cations. The earliest evidence of the former can be found among the reduced binary transition-metal halides (and sulfides) in which discrete clusters appear for the intermediate metals (Nb, Ta, and Mo). On the other side, extensions of the family of classical so-called Zintl phases to the earlier p (and late d) metals yield instead active metal salts of electron-poorer anionic clusters and nets with more delocalized bonding. Distinctive complex QCs and ACs are also found among the latter as multiply-endohedral structures in which special electronic properties (pseudogaps) appear near certain valence electron counts, in particular intermetallic systems. Of course, neither of these types originated from such foresight; rather, their discoveries and organization reflect continued interests in metal−metal bonding in extended solid-state systems, as well as persistence and serendipity.

It is easy to anticipate the discovery of much more that is new and novel. A large fraction of the possible ternary intermetallic systems, and most quaternary and higher members, have not been well examined, especially regarding numerous, unusual, unprecedented, or unimaginable compounds, structures, and properties. A large fraction of the results described here have come about in the past decade in the pursuit of synthesis, structure, and bonding in these "odd" metal-based systems.

**Acknowledgment.** The real credits for all of these accomplishments belong to many clever, curious, imaginative, and persistent co-workers; the names of many of the more recent collaborators appear in the references. The cover design was created by one of these, Professor Ling Chen at Fujian Institute (FJIRSM), Fuzhou, China. On the financial side, steadfast support from the U.S. Department of Energy (and its predecessor agencies) through the Ames Laboratory has made all of the Zintl phase and triel polyanion studies possible. In parallel, the National Science Foundation (DMR) has supported the polycation and AC/QC investigations over the last 25 years, presently by means of Grant DMR-0853732.

(66) Li, B.; Corbett, J. D. *Inorg. Chem.* **2007**, *46*, 6022.
(67) Li, B.; Kim, S.-J.; Miller, G. J.; Corbett, J. D. *Inorg. Chem.* **2009**, *48*, 6573.
(68) Li, B.; Kim, S.-J.; Miller, G. J.; Corbett, J. D. *Inorg. Chem.* **2009**, *48*, 11108.